

---

# The QED Engine: Fusion-Electric Propulsion for Cis-Oort/Quasi-Interstellar (QIS) Flight

By Robert W. Bussard and Lorin W. Jameson, Energy/Matter Conversion Corp.  
680 Garcia Street, Santa Fe, NM 87505, <[emc2qed@comcast.net](mailto:emc2qed@comcast.net)>  
and H.D. Froning, Jr., Flight Unlimited, Inc. Flagstaff, AZ

---

## Abstract

QED propulsion systems use light-weight inertial-electrostatic-fusion (IE) power sources to accelerate propellant with energy from clean fusion reactions. These can be applied to the flight spectrum from high-speed aircraft to quasi-interstellar (QIS) travel. For rocket propulsion electrical c-beams can be used for propellant heating, but QIS flight must use propellant-diluted fusion products, directed magnetically. Each engine type scales uniquely, but the thrust/mass ratio  $[F]$  varies crudely with specific impulse  $[I_{sp}] = I_{sp}/1000$  over the classes as  $[F] [I_{sp}]^{1.125} = 9.5$ , for  $0.15 < [I_{sp}] < 150$ . QIS flights are examined with special attention to missions to 100-1000 A.U.; these can be achieved with single-stage vehicles at constant power in 1.5-5 years along an acceleration/coast/deceleration flight profile, with  $200 < [I_{sp}] < 300$  sec. QIS engine design requirements are found to be within the range of practical engineering technologies.

## Nomenclature

$a_o$	= initial vehicle force acceleration
$a_f$	= final vehicle force acceleration
$B$	= magnetic field strength
$E_o$	= core ion energy in IEF system
$F, [F]$	= engine thrust, thrust/mass ratio
$G_{gross}$	= ratio gross electric to drive power
$I_{sp}$	= engine system specific impulse
$[I_{sp}]$	= normalized $[I_{sp}] = I_{sp}/1000$
$m_o$	= vehicle gross mass
$m_e$	= engine system mass
$m_p$	= propellant mass

$m_L$	= payload mass
$P_f$	= gross fusion power
$P_o, P_{rst}$	= net fusion or electric power
$P_L = P_{net}$	= propulsive jet thrust power
$t_b$	= engine thrusting ("burn") time
$v$	= vehicle speed
$v_o = gI_{sp}$	= propellant exhaust speed
$\delta S, S$	= incremental distance traversed
$\delta v_c$	= "characteristic" velocity of flight/mission

## 1. Introduction

The direct production of electric power appears possible from fusion reactions between fuels whose products consist solely of charged particles and thus do not present radiation hazards from energetic neutron production, as do reactions involving deuteron-bearing fuels. These include the fuels p ( $^1\text{H}$ ),  $^{11}\text{B}$ , and  $^3\text{He}$ . These can be "burned" in inertial-electrostatic-fusion (IEF) devices<sup>1,2</sup> to power quiet-electric-discharge (QED) fusion propulsion systems. IEF power sources can provide direct-converted electrical power at high voltage (MeV) to heat and expand or to accelerate directly a working fluid to provide rocket thrust at high specific impulse ( $I_{sp}$  from 1500 to 70,000 sec). These engine systems are most useful for near-and solar system interplanetary flights. Alternatively, the fusion products can be used to heat directly a propellant/diluent. Such a diluted-fusion-product (DFP) engine system avoids the difficulties and thermal limitations of energy conversion equipment and allows attainment of extremely high  $I_{sp}$  — up to that of the fusion products alone ( $I_{sp} \approx 1.4\text{E}6$  sec) — as required for long-range QIS missions.

Here, initial summary is given of QED fusion-direct-electric engine systems, and of their features and performance ranges. This is followed by review of the principles and characteristics of IEF power source systems, and a discussion of their application to the DFP engine concept for QIS missions. Special attention is given to vehicle performance over a range of very high specific impulse (1E5-1E6 sec) and to discussion and specification of a typical candidate DFP/IEF engine and single-stage vehicle for rapid flight to 550 A.U.

## 2. OED Engine Systems

The simplest and most direct engine system is all-regeneratively-cooled (ARC) and employs direct-electric-driven quasi-relativistic e-beams (reb) for 100% efficient heating of air or rocket propellant to extreme temperatures, with resulting high specific impulse exhaust performance capabilities.<sup>3</sup> This basic QED rocket engine configuration is shown in schematic outline in Figure 1. The upper limit performance of this ARC/QED engine is set by the maximum limiting cooled-structure temperature. Its thrust/engine-mass ratio  $[F]$  and normalized specific impulse  $[I_{sp}] = I_{sp}/1000$  scale approximately as  $[F]_{arc} [I_{sp}]^{0.85} = 8.5$ ; here higher  $I_{sp}$  improves performance (relative to the usual  $F \propto 1/I_{sp}$  scaling) because of the minimum size and mass of the smallest IEF source that can be used practically with fusion fuels of interest.

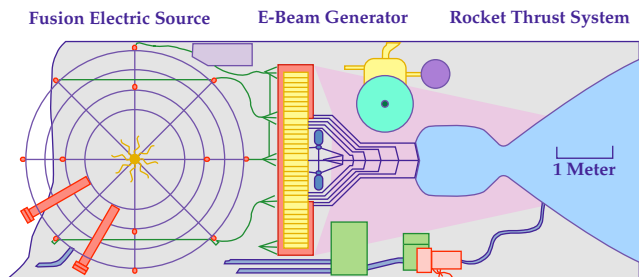


Figure 1 — Schematic outline of ARC/QED engine system

Higher  $I_{sp}$  can be attained by use of controlled space radiators (CSR), rather than regeneration, to handle the waste heat loads. However, the upper  $I_{sp}$  limit of such thermal CSR/QED (here called CSR-A) systems is, once again, thermal; here it is the limiting temperature that can be sustained by the nozzle walls. This maximum temperature, and hence  $I_{sp}$  is set by thermal radiation from the propellant gas to the walls, and this can not be inhibited by the particle-convection-insulating nozzle wall B fields. Beyond this limit it is necessary to use the IEF-generated direct-electric power to drive still higher exhaust speeds in a non-thermal manner, by means of collective acceleration in electron-beam traveling-wave fields. The performance of this (CSR-B) system is set by the absolute limit of unavoidable waste heat cooling. This is about 1E-4 of system total power, due to gamma-

and X-ray heating of cryogenic structures required for the super-conducting magnets. These CSR-A, B engine systems scale differently than ARC engines, following a more complex scaling algorithm that reflects the variable mass of waste heat radiator required as the system  $I_{sp}$  is made to increase above the ARC limiting values. This is given simply as the ratio  $[F]_{CSR} = [F]_{ARC}/[1 + (m_{rad}/m_{ARC})]$ , which can be written:

$$[F]_{CSR} = \frac{[F]_{ARC}}{1 + \left[ 2.24 / \left( \frac{T_{rad}}{1000} \right)^4 \right] I_{sp}^{0.15} \frac{[I_{sp}] - 5.5}{64.5}} \quad (1)$$

for two-sided radiation at a temperature  $T_{rad}$  (°K), with radiator single-sided surface area specific mass of 3 kg/m<sup>3</sup>. Here  $T_{rad}$  is radiator temperature in °K. Figure 2 provides schematic outlines of each of these QED engines, in sequence, showing the principal subsystems of each complete QED engine system, as described above.

Such engines can be used for missions ranging from practical ground-to-earth-orbit flight to fast flights through the inner and outer solar system, with both short flight times and high payload fractions in single-stage vehicles. The performance of such engine systems has been detailed previously<sup>4</sup> for such missions. Following the algorithms given above, the general level of performance found for this sequence of QED propulsion systems is shown in Figure 3, which plots propellant exhaust specific impulse  $I_{sp}$  as a function of engine system thrust/mass ratio  $[F]$  in comparison with performance projections for other concepts for fusion propulsion.<sup>5</sup> The ARC and CSR (with  $T_{rad} = 1100$  °K) QED engine performance curves shown are based on IEF sources using p<sup>11</sup>B fusion fuels, and are seen to outperform all other advanced concepts for controlled fusion propulsion by 2-3 orders of magnitude. The <sup>3</sup>He<sup>3</sup>He reaction can not be used practically in the ARC/CSR engine concepts because of the difficulty of direct electric conversion of the wide energy spread of its fusion products. However this is not an impediment for the thermal conversion or utilization of their energy.

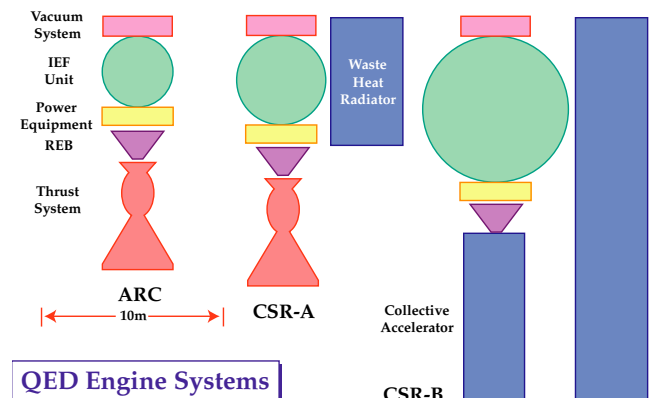


Figure 2 — Schematic outline of QED engines, from regeneratively-cooled to space radiation systems

Thus this reaction may prove useful for thermal/electrical power generation in central station power plants, when  $^3\text{He}$  fuel (eventually) becomes available from a widely-diffused space-based economy, or for use in the non-electric DFP engines of interest for QIS flight missions.

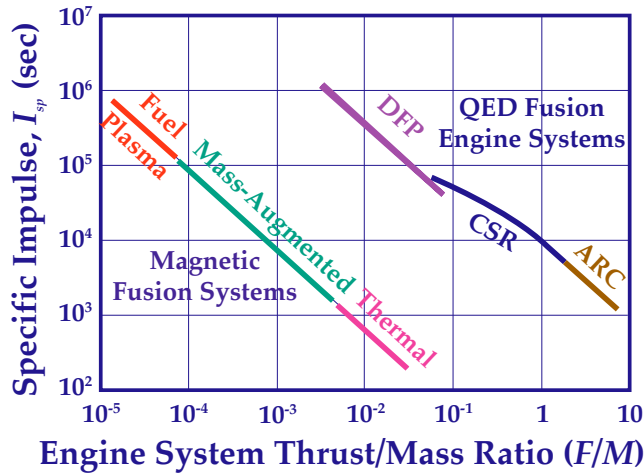


Figure 3 — QED engine performance, showing  $I_{sp}$  variation with thrust-to-engine-mass ratio  $[F]$  compared with conventional magnetic fusion concepts.

Propulsion system performance beyond even these levels is required for practical space flight to more distant, longer missions such as those to the Oort Cloud or the solar-lens gravitational point (550 A.U.), or to further quasi-interstellar distances. For such missions, the usual QED engine thermally-limited direct-electric-conversion systems must be abandoned in favor of systems that use direct-fusion-product (DFP) propellant heating, without the medium of intervening mass-accelerating machinery. The performance range of such DFP engines using  $p^{11}\text{B}$  fuel is also shown in the figure. These are discussed in more detail in following sections.

### 3. IEF Power Sources

The IEF fusion-electric source systems of interest here all use quasi-spherically-symmetric polyhedral magnetic fields to confine electrons which are injected at high energy  $E_0$ , so as to form a negative electric potential well that can confine fusion ions in spherically-converging flow. Figure 4 shows a schematic diagram of this electron-acceleration (EXL) IEF system. Fusion ions are inserted into the well near its boundary  $R$ , so that they “fall” towards the center and oscillate across the machine, with density increasing rapidly ( $1/r^2$ ) towards the center. Their injection rate is controlled (relative to electron drive current) so that their core energy reaches a specified central virtual anode height  $\eta = \delta E_0$  desired for

system operation. They reach maximum density at a core radius set by the ratio of their initial transverse energy  $dE_1$  at injection, to their energy  $E_0 = (1-\eta)E_0$  at the core boundary  $r_c$ , as given by  $\langle r_c \rangle = r_c/R = (dE_1/E_0)^{0.5}$ . Typical ion convergence ratios are  $0.001 < \langle r_c \rangle < 0.01$ , which yield core densification of  $1E4-1E6$  above the minimum ion densities in the system.

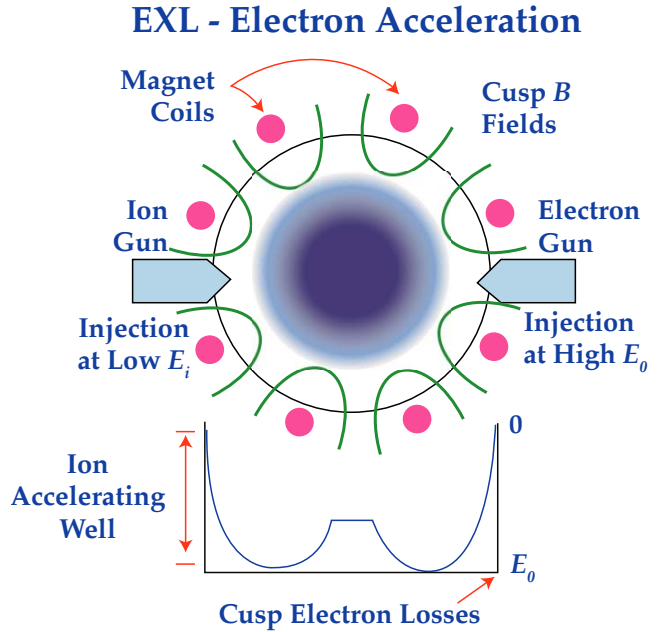
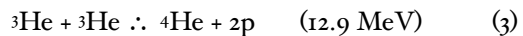


Figure 4 — The EXL/IEF concept; ion acceleration by electron-injection driven negative potential well maintained in polyhedral magnetic field

### Clean Fusion Reactions

Preferred fusion reactions are those whose products consist solely of charged particles. These reactions are free from the radiation hazards of energetic neutrons which always characterize fusion in deuterium-bearing mixtures. The clean fusion fuels of most interest for QED and DFP propulsion engine applications are  $^1\text{H}$ ,  $^{11}\text{B}$ , and  $^3\text{He}$ , reacting according to:



The direct production of electric power from these reactions is possible by deceleration of the charged fusion product ions in an externally-imposed electric field. They will move predominantly radially from their central birth point in the IEF core region, and can be collected as they approach zero kinetic energy, by grids or plates placed at appropriate radial positions along the particle path. These collectors are connected to the electrical circuit in which current is driven through the system external load. In such a direct conversion system (DCS) the easiest fusion products to direct-convert are those of (2), because of the well-defined energies of the

fusion product alphas.<sup>6</sup> These are roughly 2.46 MeV and 3.76 MeV and, since their charge is  $Z = 2$ , electric field deceleration requires a retarding potential of only about 1.9 MeV. This can be sustained by spherically-symmetric grids located at 0.5-1 m outside of the IEF ion-confining region. Thus, complete direct-conversion  $p^{11}B$  IEF systems need be only about 1-2 m larger in diameter than the size required for producing the controlled fusion process, itself.

The second reaction is much less suited to electrical power production by direct conversion because the energy distribution of the reaction products in (3) is continuous rather than discretely defined, and the proton energy can range from about 10.7 MeV to nearly zero, with a corresponding variation of alpha energy from 1.1 MeV to 6.4 MeV. Converting the maximum energy of the proton requires DCS structures of sizable radial dimensions (ca. 5-10 m), and the spread in energy forces the collection of fusion products over the entire extent of the decelerating system, thus many collection grids are required. This poses both mechanical and thermal problems considerably worse than those for the  $p^{11}B$  reaction, with its well-defined fusion product energies. Indeed, the  ${}^3He^3He$  system seems suited to propulsion use only through direct heating of propellant in a diluent/propellant system, rather than through a direct electro-conversion cycle to produce power for subsequent propellant heating.

For extremely high  $I_{sp}$  as needed for high performance in QIS flight, it is impractical to use energy conversion machinery for main power in any event, because even minor inefficiencies pose insuperable thermal loads and waste heat disposal requirements that can be met only with massive space radiator and internal cooling systems and equipment. Thus, both the  $p^{11}B$  and  ${}^3He^3He$  cycles should be employed in direct propellant heating, to achieve highest  $[F]$  for DFP engines. In the present work the  ${}^3He^3He$  reaction system is not considered further.

## IEF Vacuum System Operation and Fuel Recycling

In conventional applications, IEF sources must be maintained and operated at low background pressure ( $< 1E-7$  torr) by continuous vacuum pumping on the outer shell containing the fusion reaction region.<sup>7</sup> This will remove both unburned fuel atoms as well as the fusion products, themselves, which must then be separated for subsequent use. However, the DFP engine concept requires that the fusion products *escape* the IEF source, to expand freely into an external region in which propellant/diluent is supplied, and thus to achieve control of thrust and specific impulse by control of the mixture ratio of diluent and fusion product mass flows. The IEF system

must not be contained by a vacuum shell but must be open to the vacuum region of the propellant/diluent mixing region which, itself, is open to space as its main vacuum pumping system. However, some means must be found to capture and reuse unburned fuel before it reaches the mixing region, else this will also be lost to space along with the fusion products and diluent exhaust. Fortunately, it is relatively simple to capture unreacted fuel ions, because their energy is very small compared to that of the fusion products, and their internal orbits across the system are quite constrained.

Fuel ions that are upscattered in energy by core collisions after sufficient residence time in the IEF system (without fusing), will circulate to greater and greater radial extent as their energy becomes larger and larger. A porous tungsten tube surrounded by a solenoidal magnetic field with axis radial to the system center, can be placed at such an outer radial position. This "limiter" will then be struck by and will adsorb these energetic ions when they have reached the radial position of the limiters. Vacuum pumping of the limiter will then extract the captured fuel ion — now neutral atoms — and allow them to be recycled back into the IEF system for subsequent use. Design studies of such limiters show that they need occupy only about 0.001-0.01 of the IEF active surface at the magnet radius, thus will not impose a significant power loss on the system. By use of this IEF device geometry and limiters, the separation of fusion products from unburned fuels can be accomplished in a straightforward manner with a minimum of external equipment, resulting in an IEF source ideally suited to DFP engine use.

## System Configuration Thermal Loads and Fusion Power Output Performance

In the DFP engine application, the IEF source configuration is very much simpler than for use in QED/ARC/CSR engines, or in any other central station power system. This is precisely because there is no external vacuum shell directly surrounding the fusion reactive region, thus eliminating the need for structure and cooling of such a shell. Here the magnet coils define the active radial boundary ( $R$ ) of the source, and are the main structures of the unit. Consider a truncated cubic magnet array. Here the driving electron guns are mounted at about 1.15  $R$  on radial rods extending in from the DFP engine system external confinement/thrust shell. The IEF magnets are held in place by mutual interconnects and mounted from the external shell on radial support struts that supply the electric current to drive the magnets and on support cylinders that supply the  $p^{11}B$  fuel to neutral gas sources that feed the IEF system. The general arrangement of the IEF unit and the external

confinement/thrust shell in the DFP engine is shown in Figure 5.

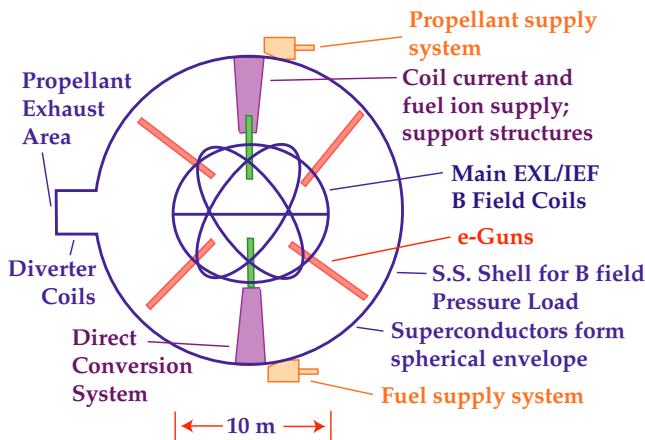


Figure 5 — Schematic outline of DFP engine, showing IEF placement, confinement/thrust shell, and magnetic diverter exhaust “nozzle;” thrust is to the right

The only unavoidable waste heat that must be removed is that from the magnet coil containers, the electron injection guns of the system, the decelerating grids of the DCS structures, and the thrust shell surface that “sees” bremsstrahlung from core electrons. The only thermal power load on the magnets is that from core bremsstrahlung; escaping fusion product ions can not strike the magnets because their fields are so high that they are magnetically insulated from such impact. The e-gun load is due to electron leakage through the magnet cusps, and the only DCS heating is due to impact of fusion products on the collection grids with the residual energy left *after* direct conversion has taken place. However, note that the DCS system for the DFP engine is very small, as it need supply only the IEF drive (injection plus bremsstrahlung) power; it is not used to convert the bulk of the fusion energy as in a direct-electric QED engine. Typically, the DCS system here will convert about 0.024 of the total fusion power to drive the fusion system, itself.

The bremsstrahlung thermal load on the magnets is that of the geometric intercept fraction of the magnet coils, while the DCS post-converter load depends on the excess energy allowed to the fusion ions after passing through the electrical deceleration portion of the converter. For the  $p^{11}B$  fusion reaction this can be kept to less than 50 keV (out of 2.5-3.8 MeV), limited only by the energy spread introduced by the confining potential well depth. Typically, the magnet geometric intercept fraction can be kept below about 0.05 of the “all-sky” area, while the DCS grid intercept area fraction can be as small as 0.025. Thus the magnets can intercept only 5% of the bremsstrahlung, while the remaining 95% is deposited on other structures (e.g. the e-guns) or the thrust shell. All of the bremsstrahlung thermal load must be cooled and radiated to space to preserve the high- $I_{sp}$  potential of the DFP engine. Similarly, all of the

electron injection power eventually must be cooled and radiated to space, as must that fraction of fusion product power not converted in the DCS. The external shell is insulated from residual charged particle kinetic power by a strong magnetic field supplied by a large axial current flowing through the shell, as described below.

The electron injectors must supply the current needed to drive operation of the EXL fusion stem in the “wiffleball” (WB) electron diamagnetic mode.<sup>8</sup> This required injection current is reduced by an e-gun electron reflectance factor of  $(1-\alpha_R)$ ; typically  $\alpha_R = 0.9$ . This power must be taken as waste heat, from cooling of the gun grids and the internal limiter structures at the ion-confining radius. However, the *total* electron power injected must also include the bremsstrahlung power, which can be supplied only by electron input. In these IEF systems fusion energy can not drive the bremsstrahlung, as it can in large, equilibrium magnetic confinement machines.

To estimate heat loads and output performance of such IEF sources, it is necessary to determine the gross fusion power, net power output, gain, drive power and bremsstrahlung power for their operation. This has been done over a wide parametric range for many fuels, using the complex power balance code (PBAL), developed since 1990 for such analyses. Limiting interest to  $p^{11}B$ , Figure 6a,b shows an example of performance for the reaction of (2), for  $\alpha_R = 0.9$  and other parameters as shown on the figure.

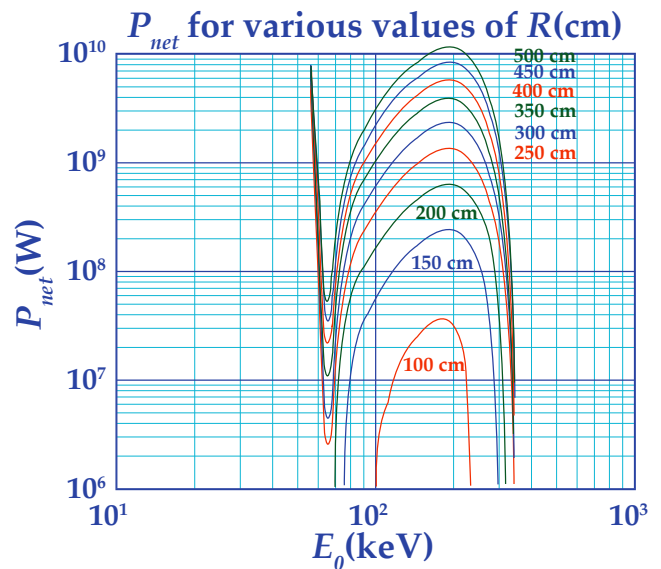


Figure 6a — Fusion power for  $p^{11}B$  IEF system

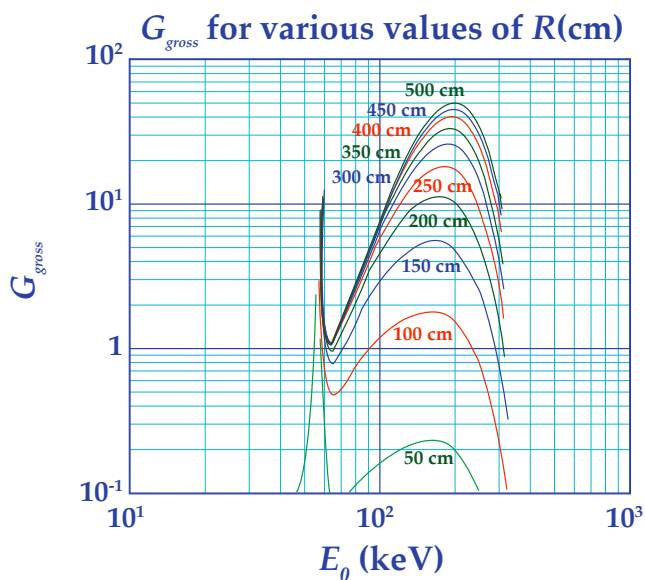


Figure 6b — Fusion gain for p<sup>11</sup>B IEF system

Consider a source with a fusion-ion-confining radius of  $R = 5.0$  m, driven electron injection at 220 keV and operated with an ion convergence ratio of  $\langle r_c \rangle = 1E-3$  at a virtual anode height fraction of  $\eta = 1E-3$ , with a  $B$  field of 13.5 kG at  $R$ , provided by super-conducting magnets. For these parameters the IEF device of Figure 6a,b will yield gross fusion power of  $P_{fus} = 10,245$  MW at a gross gain ( $P_{fus}/P_{drive}$ ) of  $G_{gr} = 46.3$ . This gives an electron drive power (injection plus bremsstrahlung) of  $P_{drive} = 221$  MWe. Assume that the direct convertor grids subtend 0.05 of the DCS surface as viewed from the IEF core, and allow 70 keV spread in the convertor deceleration process for a deceleration conversion efficiency of 0.95. Then, the complete conversion efficiency of the DCS will be 0.90. The remaining 0.10 of unconverted power into the DCS must be radiated as waste heat. Since 1 MWe is needed to drive the machine, the DCS must accept a fusion power of 245 MW<sub>fus</sub>, or about 0.024 of the gross fusion power produced. For use of dual, oppositely mounted DCS systems, this requires a DCS acceptance solid angle fraction of 0.012, which is obtained through a 2.19 m radius hole at the external shell radius of 10 m from the IEF core center. The total waste heat load is also this 245 MW<sub>th</sub> (drive and DCS waste heat), which must be dumped to space through a waste heat radiator. Note that if the fusion power were to be converted in entirety at the DCS efficiency, the system would produce a net electric power of  $P_{net} = 9000$  MWe.

With full waste heat space radiation, the system is limited only by the maximum propellant specific impulse associated with expulsion of the fusion product alpha particles from p<sup>11</sup>B fusion. These leave with speeds of 2.2-2.7E9 cm/sec for a particle-weighted average speed of 2.4E9 cm/sec. Assuming particle escape from the IEF source with a distribution characteristic of a diffuse

emitter from the external confinement/thrust shell exit hole, the average effective specific impulse would be about  $I_{sp} = 1.2E6$  sec or  $[I_{sp}] = 1200$ . Regenerative cooling is not used for any significant purpose in this system. Lower  $I_{sp}$  can be attained only by reducing the mean energy per particle by mixing the fusion alphas with diluent atoms/ions. Independent of the choice of diluent (i.e. water or ammonia are as useful as monatomic hydrogen; this is not a temperature-limited system), the net effective  $I_{sp}$  of the mixture is given simply by  $I_{spmix} = I_{spo}/(1+D)^{0.5}$  where  $I_{spo}$  is the undiluted specific impulse (1.2E6 sec, above) and  $D$  is the diluent mass flow ratio. For example, if the mass flow rate of diluent is taken to be three times that of the fusion fuels, then the resulting specific impulse will be one-half of  $I_{spo}$ . At large dilution ratios the  $I_{sp}$  varies as  $1/D^{0.5}$ , so that 10,000:1 dilution yields  $I_{spmix} = 12,000$  sec, under the above assumptions.

## 4 DFP Engine System: Features and Requirements

The thrust/mass ratio attainable in the DFP system is determined by the masses of all of the subsystems of the complete engine system. First of these is the EXL/IEF unit, itself, consisting of the magnet coils, e-guns and power supplies, cryogenic cooling and limiter vacuum systems, fuel feeds, and support structures. These must be driven by electrical power provided by the DCS, which includes the grids and standoff structures, and current leads to the IEF loads (e-guns and magnets). The propulsion thrust subsystem is based on the external (to the IEF unit) plasma confinement/thrust shell. This is toroidal, with super-conducting current carriers to provide the toroidal field that confines the diluent ions and fusion products until they reach some measure of energy equilibration. It also includes the propellant/diluent feed system and pumps and associated support structures. Finally, the mass of the waste heat radiator must be included. Figure 5, previously, gives the arrangement of subsystems in the DFP engine, and Figure 7 shows the current paths and resulting  $B$  field distributions in the engine system external to the IEF unit.

### EXL/IEF Unit and Toroidal Confinement Shell

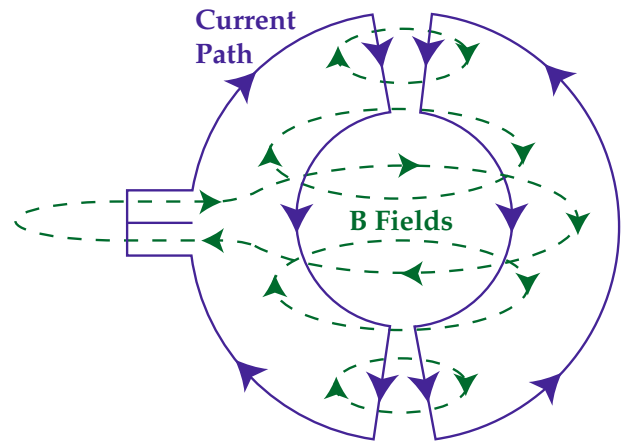
The mass of an EXL/IEF unit for use in the DFP engine will be determined principally by its magnet coils that bound the active fusion system radius,  $R$ . Since there is no confining vacuum shell around the EXL unit, the only other masses of note are those of the e-guns, ion supplies, and support structures to hold the unit in place within the external thrust shell. The magnet mass is determined entirely by its volume, and this is set by the current required to produce the necessary  $B$  fields and the fixed maximum current density ( $K_c$ , amps/cm<sup>2</sup>) that

can be utilized by the superconductors that make up the magnet coils. A true spherical polyhedral truncated-cube field configuration uses four identical coils, each of radius  $R$ , intersecting as the projection of the truncated cube bounded by their spherical surface. For a 13.5 kG machine with a 5m radius, the current required is about 15.3 MA (1.53E7 amps) in each of the coils. If the coils can be run at  $K_d = 50$  kA/cm<sup>2</sup>, for example, the conductor cross-section must be 305 cm<sup>2</sup>. Since the total coil length is  $8\pi R$  and its density is about 5.8 gm/cm<sup>3</sup>, the coil mass is found to be 22,230 kg.

The external thrust shell, which is spherical, constitutes the conducting boundary of a toroidal magnetic field whose configuration allows the controlled confinement of both fusion products and diluent ions until their escape through an exit hole to provide thrust. This exit hole or “nozzle” is formed by external field coils that create a “bundle” divertor for confined plasma. Such divertors have been used in tokamak magnetic confinement research. The parameters that define the size of this escape hole are all controllable by design, being determined by the magnetic field required for the toroidal confinement system, the field needed to divert the primary toroidal field and establish the desired size of exit “nozzle” hole, and the  $I_{sp}$  desired from the propellant mixture. Note that the toroidal geometry is quite similar to that of classical tokamak fusion concepts, without the poloidal field, but that the fields needed here for adequate confinement are less than those used in such machines by the square root of the ratio of energy exchange Coulomb collision cross-sections to fusion-reaction cross-sections (ca. 1000x).

This shell embodies two structures. One is the superconductors that carry current to generate the outer section of the toroidal magnetic field and the other is a thin, spherical skin of high-strength steel to carry the magnetic pressure load of these conductors. The fields insulate the shell from impact by the fusion products and heated propellant ions. For good field coverage of the surface, the design here uses 360 conductors spaced at one degree intervals (about 17.5 cm at the equator) that are made of 1.04 cm diameter superconductor cable. Each cable carries 42.5 kA and is contained in leak-tight steel tubing outside the skin to allow passage of cryogenic cooling fluid to maintain superconductor temperature. These external superconductors converge (to about 3.5 cm spacing) as they approach the torus axis, and close the current loop through paraxial conically-arranged conductors that connect from the shell surface radius to the IEF main coil feed system. These conical conductor sets (one at each end of the torus axis) support the IEF and bound the DCS volume at each end of this support system. The total mass of the conductors on the shell and return cones (exclusive of IEF coils) is 11,470 kg.

The simplest way to design the electrical/magnetic system is to use the same current for both the IEF  $B$  field coils and the shell superconductors. This will give a  $B$  field at the mean shell radius of about 8.2 kG, and a surface field of 4.1 kG. If higher shell fields are desired, the shell current can be doubled, while maintaining the same IEF  $B$  field strength by splitting the current as it feeds these coils. This will keep the main  $B$  field coil mass the same but result in doubling the shell superconductor mass and increasing the shell steel skin mass by a factor of four. The lower shell fields seem adequate, as the gyro radius of fusion alphas is only about 12.2 cm at the shell mean radial field. Thus, the IEF-to-shell spacing is ca. 41 gyro radii at fusion energies, allowing about 1700 effective energy exchange collisions before permitting alphas to reach the wall. This collisionality far exceeds that needed to equilibrate the alphas with the propellant (or to control escape of the alphas, if no diluent is used) that higher shell currents and fields seem unnecessary. Figure 7 shows the arrangement of current paths and resulting  $B$  fields.



### Current Flow and Toroidal B Field Configuration

Figure 7 — DFP engine current and B field configurations

Exact determination of the toroidal field strength required in the DFP engine can be done only by analysis of the collisional interactions that produce fusion alpha slowing-down by Coulomb collisions with the inflowing propellant/diluent, which is injected in the high-field annular region around the DCS/torus-axis. The field strength will affect this three-dimensional flow and collision process in the subsequent motion of these particles towards their escape at the exit divertor field region of the torus, but such a complete analysis is beyond the scope of the work reported here. However, some illustrative features of this process can be shown by examination of the conditions for particle escape through the “nozzle” hole as set by plasma/ $B$ -field confinement.

## Engine Plasma Exhaust Flow and Thrust

The total mass flow out of the exit hole is just the product of the plasma density  $n_{e,i}$  at the exit surface, the plasma ion mass  $m_{e,i}$ , the exit speed ( $0.707 v_i$ ), and the hole area  $A_{ex}$ . Multiplying this by the average exit speed (mean specific impulse) of the escaping mixture yields the system thrust. But the thrust times the exit speed is just the system power, which is held fixed in this analysis. Finally the necessary remaining relationship between exit plasma density and the toroidal  $B$  field is found from the pressure balance  $p = nE = \beta B^2/8\pi$ , where  $\beta$  is the usual plasma “beta” parameter. This is simply the ratio of kinetic pressure to magnetic pressure at the exit plane. Combining all of these yields an equation for the size of exit hole required as a function of the system power, fusion alpha particle energy, diluent mass flow mixture ratio ( $D$ ), plasma  $\beta$ , and the surface  $B$  field  $B_{ex}$ . This equation incorporates all of the relevant physics inter-relationships of the system and is:

$$A_{ex} = 1.04 \sqrt{\frac{D}{E_\alpha}} \left( \frac{P_{fus}}{\beta B_{ex}^2} \right)_{(4)}$$

Here the area is given in  $\text{cm}^2$  if  $E_\alpha$  is alpha energy in MeV,  $P_{fus}$  is in MW, and  $B_{ex}$  is in kG (kilogauss). As an example, consider a system with  $P_{fus} = 10,000$  MW,  $E_\alpha = 4$  MeV, with  $D = 25$  and a plasma beta of  $\beta = 0.03$  (typical). For these parameters the exit hole “nozzle” escape area will be  $A_{ex} = 0.867E6/B_{ex}^2 \text{ cm}^2$ . If  $B_{ex} = 4.1$  kG, as for the current flow conditions used above, this gives  $A_{ex} = 5.156E4 \text{ cm}^2$ , for a hole radius of about 128.1 cm. Figure 5 shows such a thrust area at the equatorial divertor region.

## Electrical Power Supply and IEF System Mounting

The DCS mass is small (for a  $p^{11}\text{B}$  fusion system) simply because it is converting only about 2.4% of the total system power, and it is not large in size because it can operate reliably at a voltage gradient of 1.5 MeV/m, and the maximum convertor voltage required for  $p^{11}\text{B}$  alphas is only 3.8 MeV. For the dual axially-mounted DCS configuration, the acceptance hole area needed for this power fraction is about 2.2 m in radius, and the standoff distance for the convertor grids is about 2 m. This acceptance radius reduces to 1.1 m at the IEF boundary. The shell return current conductors carry the full drive current through a conical conductor arrangement, delivering current to the distribution coil that feeds the main IEF coils. A similar arrangement takes the current out of the IEF at the opposite end and returns it to the shell conductors. The IEF device is mounted so as to present

a triangular face to the DCS units. This face area is about 6% of the total sphere area, thus each DCS free flow area fits well within the small dimensions of these triangular polyhedral faces. The EXL unit, itself is supported from the edge of the DCS hole by the return current conductors, each carrying current to the e-guns and to the main coils from the electric power system supplied by the DCS.

Three additional structural columns also carry the  $p^{11}\text{B}$  fuel gas (as diborane,  $\text{B}_2\text{H}_6$ ) to the ion or neutral gas injection system that fuels the unit. Natural boron can be used, as this is over 80% boron-11; thus avoiding the need for isotopic separation of the fusion fuel. Other supports are associated with the placement of the e-guns on each of the main (square) faces. These are all mounted on radial spokes extending from the surface shell support structure. Estimates give about 2290 kg for the mass of the complete electric system, including dual power conditioning and DCS structures. A  $^3\text{He}^3\text{He}$  DCS system using protons with maximum energy of about 11 MeV would be about 8.7 times larger in mass than a  $p^{11}\text{B}$  system of the same total power.

## Waste Heat Radiator and Cryogenic Cooling System

All of the 221 MW of electrical drive power and 24 MW of unconverted particle power in the DCS must be disposed of as waste heat, to avoid  $I_{sp}$  limitations from regenerative cooling. Thus, a space radiator capable of handling 245 MW of radiated power is required. Since the radiator mass is just the product of its area  $A_{rad}$  and its specific area density  $P_{rad}$  its mass is fixed by the choice of radiating temperature, for any given emissivity. Using the usual formulas  $P_{rad} = \epsilon\sigma T_{rad}^4$ , where  $\sigma$  is the Stefan-Boltzmann radiation constant ( $5.67E-12 \text{ w/cm}^2\text{K}^4$ ), and a specific mass of  $3 \text{ kg/m}^2$  (single-sided) while allowing double-sided radiation, and taking a radiator temperature of 1050 °K, the radiator mass of the example DFP engine system is found to be only 5290 kg.

Similarly, taking 70 watts of electric drive power as required for each watt of cryogenic cooling power, and limiting this to the unavoidable minimum due to gamma- and X-ray heating of the superconductor coils and conductors, it is found that the total cryogenic heat load is about 50 kWth. For this, the cryogenic system drive power must be about 3.5 MWe, all of which must be dumped to space via a radiator system. By analogy with the main space radiators, above, the cryogenic system radiators will have about 800 kg mass. The cryogenic pump mass is estimated to be 1600 kg, and the power supply for these is taken at 0.5 kg/kWe as 1750 kg for a cryogenic system hardware mass of about 4150 kg. The complete system must also include fluids stored and

used over its life; this is estimated to be about 350 kg for a total mass of 4500 kg.

Other masses include the six e-guns, estimated at 840 kg the propellant/diluent (LH<sub>2</sub>) supply pump system estimated at 500 kg; and the p<sup>11</sup>B fueling system, including pumps, ion guns/injectors, and limiters, taken as 1000 kg. These and all the other system masses are summarized in the Table 1.

## Summary of System Mass

**Table 1 — System/Subsystem Masses for DFP Fusion Rocket Propulsion Engine**

Subsystem	Estimated Mass	Comment
Radiator, $m_{rad}$	5,290 kg	3 kg/m <sup>2</sup> ; 1050 K
Misc., $m_{misc}$	1,320 kg	
Cryogenic cooling system, $m_{cryo}$	4,500 kg	70 W/cryo-W
Shell, $m_{sh}$	2,950 kg	4.1 kG B field
Engine S/C, $m_{sc}$	11,470 kg	At 50 kA/cm <sup>2</sup>
IEF B field coils, $m_{ief}$	22,230 kg	At 50 kA/cm <sup>2</sup>
Fusion fuel system, $m_{pB}$	1,000 kg	
Diluent System, $m_{LH}$	500 kg	
Electrical power system, $m_{elect}$	2,290 kg	At 10 kg/MWe
e-guns, $m_{eg}$	840 kg	6 @ 140 kg
Total	52,390 kg	

## 5 OIS Vehicle Flight Performance

### Engine Specific Impulse

Such an engine system offers very advanced performance for long-rang space flight missions. Typically, a single-stage space vehicle of practical construction can allow about 1/e of its full mass as empty mass after propellant

expulsion. Such a vehicle will give a characteristic velocity change increment during powered flight of  $\delta v_c = g I_{sp}$ . Larger total flight velocity increment can be achieved only by use of successive stages, each providing another  $\delta v_c$  from its own propulsive action. But, multi-stage vehicles compound the overall vehicle system mass-ratio in an exponential fashion. Thus, systems beyond one stage rapidly become very unattractive due to the extreme mass growth required to attain flight speeds markedly in excess of the “characteristic” speed set by  $g I_{sp}$ . For this reason, interest here is restricted to single-stage vehicles only. This limits flight to missions that can be accomplished within the range of  $v \delta v_c = g I_{sp}$  values attainable with the DFP engine.

The maximum  $I_{sp}$  possible from the DFP engine is about 1.2E6 sec for expulsion of the fusion product alphas, alone, with a sine<sup>2</sup> angular distribution at the engine diverter exhaust plane. A lower limit also exists, set by the maximum plasma density that can be sustained within the confinement/thrust shell with tractable engine B fields and maximum allowable plasma densities external to the IEF unit. This is about at a dilution ratio of  $D = 200$  or so; larger dilution gives higher thrust and lower  $I_{sp}$ , but may begin to affect IEF operation, and gives lesser performance than the CSR-B engine system, anyway. Thus the useful and interesting range of dilution ratios in the DFP engine is  $1 < D < 200$ . The specific impulse varies with the mass dilution ratio as  $I_{sp} = I_{sp0}/(D+1)^{0.5}$ , where  $I_{sp0}$  is the specific impulse for no dilution, as above. For the range of  $D$  just given, the resulting range of  $I_{sp}$  is  $1.2E6 > I_{sp} > 7E4$  sec, thus the corresponding range of useful single-stage mission flight velocities is  $1.2E9 > \delta v_c > 7E7$  cm/sec or from 700-12,000 km/sec. Since one Astronomical Unit (AU) is about 1.5E13 and there are 3.15E7 seconds in a year, this velocity range is equivalent to a speed range of 147-2520 AU/year. It is clear from this that the DFP engine offers promise for distant sub-stellar missions.

### Continuously Accelerating Flight

The potential for QIS flight can be most simply analyzed by noting that the engine system power will be constant at its maximum value in any optimum operation. Furthermore, although minimum time trajectories may be constructed with variable  $I_{sp}$  and constant power, it is always found that maximum payload or dry mass fraction is attained, for any given flight speed increment by use of maximum  $I_{sp}$  throughout the flight. Thus, the analysis can be made on the basis of fixed power and specific impulse. For these conditions, propellant consumption rate and engine thrust are fixed throughout the flight. Assuming that the flight profile is in field-free space allows ready integration of Newton's equations for

particle motion under constant force with changing acceleration.

For a rocket vehicle with propellant mass  $m_p$  equal to  $1 - (1/\epsilon) = 0.632$  of the gross mass  $m_0$  at start of flight, the vehicle final speed (or characteristic velocity increment) will be  $gI_{sp} = \tau_e$ , the exhaust velocity of the propellant. Given fixed engine power and constant  $I_{sp}$ , the flight time during engine operation will be  $t_b = (gI_{sp}/a_0)(m_p/m_0) = 0.632(gI_{sp}/a_0)$ , where  $a_0$  is the initial force acceleration of the full vehicle. Similarly, flight distance under thrusting power is found to be  $s_b = (\tau_e^2/a_0)(1 - 2/\epsilon) = 0.264(\tau_e^2/a_0)$ . To assess actual performance for any desired  $I_{sp}$  it is thus necessary to choose a vehicle initial mass and engine power (or ratio of power to vehicle mass; noting that  $a_0 = 2P_{fus}/m_0g^2I_{sp}$ ). For illustrative purposes take  $P_{fus} = 10,000$  MW, as previously discussed for the example DFP p<sup>11</sup>B engine system (burns 0.144 gm/sec of p<sup>11</sup>B), and assume that  $m_0 = 400,000$  kg. Then flight performance for various  $I_{sp}$  values will be as shown in Table 2, following.

From this note how rapidly the flight “burn” time changes with  $I_{sp}$ , as does the p<sup>11</sup>B fuel consumed, and the distance traversed in powered flight. Note, also, that even though this example is only of a single-stage (1/ε) vehicle, the highest  $I_{sp}$  version is nearly (but not quite) a starship, covering a distance of 0.56 light years (LY) in its thrusting time of 40.1 yrs. This really astonishing performance is a direct result of the extremely high power/mass ratio of the DFP engine, and of the use of its fusion products to provide direct thrust through the medium of the toroidal-field-constrained thrust shell of the DFP system. However, since the vehicles in these examples are all moving at maximum speed at propellant burnout, they are not practical contenders for realistic flights involving human crews or scientific payloads for emplacement at distant observation points (e.g. in the Oort Cloud).

**Table 2 — Summary of Accelerating QIS Flights with DFP Engines**

### All Flight Profiles

$I_{sp}$	1E+06	3E+05	2E+05	1E5 sec
$D$	0.44	15.0	35.0	143
$F$	200	667	1000	2000 kg
$a_0$	0.5	1.667	2.5	5.0 cm/sec <sup>2</sup>
$dm_p/dt$	0.2	2.22	5.0	20 gm/sec
$m_{fuel}$	181.6	16.35	7.26	1.82 T

## Continuously-Accelerating Flight Profile

$t_b$	40.1	3.61	1.605	0.401 year
$s_b$	35,200	951	281.8	35.2 AU (0.56LY)
$\tau_{vb} = \tau_e$	2100	630	420	210 AU/year
$gI_{sp}$	c/30	3000	2000	1000 km/sec

## Acceleration/Coast/Deceleration Flight

Of greater interest are missions in which the vehicle is accelerated to half of its total velocity increment capability, coasts a portion of the flight distance, and then decelerates to zero space-frame speed once again, so that its passengers or payloads can be disembarked or fixed at a pre-chosen point in space. Analysis of such acceleration / coast / deceleration flights is somewhat more tedious than for the simple acceleration profiles of Table 2, but still straightforward because of the unique optimal operational conditions for the DFP engine. Following the previous arguments, integration of Newton’s force equations gives simple formulas for flight time and distance during the acceleration and deceleration phases of flight. These are:

Acceleration	$s_{b1} = 0.0902 (\tau_e^2/a_0)$	$t_{b1} = 0.3935 \tau_e/a_0$
Flight	$m_{pl} = 0.3935 m_0$	$m_{b1} = 0.6065 m_0$
Coast	$\tau_{coast} = \tau_e/2 = gI_{sp}/2$	
Deceleration	$s_{b2} = 0.06465(\tau_e^2/a_0)$	$t_{b2} = 0.2387 \tau_e/a_0$
Flight	$m_{p2} = 0.2387 m_0$	$m_{b2} = 0.3678 m_0$

Using these formulas, flight performance over the same range of  $I_{sp}$  as that of Table 2 was calculated for these stationary-end-point missions. The results are summarized in Table 3, which shows a variety of flight parameters for all flight phases, and gives total flight times for a mission to 557.4 AU. The first six parameters ( $I_{sp}$  through  $m_{fuel}$ ) of Table 2 apply to all QIS flight profiles for the assumed engine conditions; these are not repeated in Table 3. Inspection of the table shows that an optimum  $I_{sp}$  exists that will minimize the flight time for this (or any other) mission, and that this lies somewhere between 200,000 and 300,000 sec. Since the variation of flight time with  $I_{sp}$  is quite flat in this range, for the 557.4 AU mission, its precise choice is not critical. The dilu-

tion ratio varies from  $D = 0.44$  to  $143$  over the range of the table, and from  $15$  to  $35$  as  $I_{sp}$  changes from  $300,000$  sec to  $200,000$  sec. Note also, that the coast velocity is directly proportional, and the total burn time is inversely proportional to the  $I_{sp}$  as the fuel burn rate and thrust power are fixed.

**Table 3 — Summary of Acceleration/Coast/Deceleration Flights with DFP Engines**

$I_{sp}$	1E+06	3E+05	2E+05	1E5 sec
$s_{b1}$	12,027	324.7	96.2	12.0 AU (0.191LY)
$t_{b1}$	24.98	2.248	0.999	0.250 yr
$v_{b1}$	1050	315	210	105 AU/yr
$s_{coast}$	N/A	0	392.2	536.8 AU
$t_{coast}$	N/A	0	1.783	5.112 yr
$s_{b2}$	8620	232.7	69.0	8.6 AU (0.137LY)
$t_{b2}$	15.15	1.364	0.606	0.152 yr
$s_{btot}$	20,647	557.4	165.2	20.6 AU (0.328LY)
$t_{tot}$	40.13	3.612	3.388	5.514 yr

The mass distribution of such a vehicle is also of some interest. Consider the system with  $I_{sp} = 200,000$  sec. This has a dilution ratio of  $D = 35$ , thus its propellant is largely (hydrogen) diluent, and its structure mass is principally that of the propellant tankage. This need not withstand high accelerations, as these are never greater than  $0.01g = 10$  cm/sec<sup>2</sup>, or so, thus this can be assumed conservatively to be 10% of the propellant mass. Then the mass distribution of the example vehicle system will be:  $m_o = 400,000$  kg is gross mass,  $m_p = 252,500$  kg is propellant mass, of which  $m_{pB} = 7,260$  kg of p<sup>u</sup>B fusion fuel and  $m_H = 245,240$  kg is propellant diluent,  $m_{str} = 25,280$  kg is propellant tankage and associated structure,  $m_e = 51,705$  kg is DFP engine, and  $m_L = 70,215$  kg, or 17.6%, is left for payload, guidance, electronics, instruments, etc. This is a very high payload fraction for a single-stage vehicle on such a mission, and illustrates the potential of the DFP engine.

## 6 Conclusions

It is evident that p<sup>u</sup>B DFP engine systems can be used to achieve truly astonishing vehicle performance for quasi-interstellar flight missions. To do so requires that

they operate with dilution ratios in the range of  $10-40$ , and with EXL/IEF power sources operating on p<sup>u</sup>B fusion at power levels of the order of  $10,000$  MW. Such a source will be about  $5$  m radius, and the DFP engine system that it powers will be roughly  $10$  m in radius around the IEF source. Such engines outperform all other advanced concepts for controlled fusion propulsion by about 2-3 orders of magnitude. This advanced, innovative space propulsion system can provide very rapid transit for QIS missions, with high payload fractions in single-stage vehicles, and could allow practical mission flight times to the Oort Cloud or to, the solar gravitational-lens point, for further scientific studies.

Use of the DFP engine for true interstellar travel is also possible, although flight times will be inherently long, even with use of multistage vehicles, because the “characteristic velocity” for accomplishment of such missions over a period of 5 years, say, is about one light year per year. This is equivalent to a propellant exhaust velocity of  $c$ , the velocity of light, or a specific impulse of  $3E7$  sec. And this can not be reached with any rocket system using mass expulsion for reaction drive. The DFP engine represents the upper performance end of the spectrum of advanced rocket propulsion engines based on the inertial-electrostatic-fusion power source concept. The full spectrum seems capable of providing means for practical spaceflight from ground-to-earth-orbit, to cis-lunar, interplanetary and quasi-interstellar flight missions; all with single-stage vehicles with relatively large structure factors and payload fractions. Further development of the basic IEF source can open the door to this vision of practical spaceflight.

## Acknowledgments

This work was supported in part by the SDIO Innovative Science and Technology Office (ISTO) through the NASA Lewis Research Center (LeRC) under Contract NAS3-26711, and in part internally by Energy/Matter Conversion Corporation (EMC2). The authors wish to express their appreciation to Drs. Dwight Duston and Len Caveny (SDIO/ISTO) and to Dr. Harvey Bloomfield (NASA LeRC), for their continuing interest in and support of this work.

## Revision History

Presented at the 44th Congress of the International Astronautical Federation, October 16-22, 1993, Graz, Austria, IAA.4.1-93-708.

Reformatted and color illustrations added May 2007 by Mark Duncan. Minor updates to equations and illustrations December 2008. Slight updates to references in April 2009.

## References

<sup>1</sup> Robert W. Bussard, "Some Physics Considerations of Magnetic-Electrostatic Confinement - A New Concept for Spherical Converging-Flow Fusion." *Fusion Technology*, Volume 19, March 1991, p.273

<sup>2</sup> Nicholas A. Krall, "The Polywell: A Spherically-Convergent Ion Focus Concept," *Fusion Technology*, Volume 22, Aug. 1992, p.42

<sup>3</sup> Robert W. Bussard, "The QED Engine System: Direct-Electric Fusion-Powered Rocket Propulsion Systems," Paper #263, Proceedings of the Tenth Symposium on Space Nuclear Power and Propulsion, Albuquerque, NM, 10-14 January 1993

<sup>4</sup> Robert W. Bussard and Lorin W. Jameson, "The QED Engine Spectrum: Fusion-Electric Propulsion for Air-Breathing to Interstellar Flight," Paper #AIAA 93-2006, 29th Joint Propulsion Conference, Monterey, CA. 28-30 June 1993

<sup>5</sup> John F. Santarius, "Magnetic Fusion Energy and Space Development," Proceedings of the 24th Intersociety Energy Conversion Conference, IEEE, Volume 5, p. 2525; 1989

<sup>6</sup> Robert W. Bussard and L.W. Jameson, "Design Considerations for Clean QED Fusion Propulsion Systems," Paper #086, Proceedings of the Eleventh Symposium on Space Nuclear Power and Propulsion, Albuquerque, NM, 9-13 January 1994

<sup>7</sup> Robert W. Bussard, "Preliminary Study of Inertial-Electrostatic-Fusion (IEF) for Electric Utilities Power Plants," Final Report, EPRI Contract #RP-8012-16, Energy/Matter Conversion Corp., EMC2-0693-01, June 1993

<sup>8</sup> Robert A. Gross, "Fusion Energy," John Wiley & Sons, Inc., New York, p.134 ff; ISBN 0-471-88470-7